Satellite-based high latitude snow volume trend, variability and contribution to sea level over 1989/2006

Sylvain Biancamaria, Anny Cazenave, Nelly Mognard, William Llovel, Frédéric Frappart

Satellite-based high latitude snow volume trend, variability and contribution to sea level over 1989/2006

Sylvain Biancamaria [1, 2, 3, *], Anny Cazenave [1, 2], Nelly M. Mognard [1, 2], William Llovel [1, 3] and Frédéric Frappart [4]

[1] Université de Toulouse; UPS (OMP-PCA); LEGOS; 14 Av. Edouard Belin, F-31400 Toulouse, France

[2] CNES; LEGOS, F-31400 Toulouse, France

[3] CNRS; LEGOS, F-31400 Toulouse, France

[4] Université de Toulouse; UPS (OMP-SVT); LMTG; 14 Av. Edouard Belin, F-31400 Toulouse, France

[*] Corresponding author: sylvain.biancamaria@legos.obs-mip.fr (Phone: +335 61 33 29 30; Fax: +335 61 25 32 05)

Abstract

Snow volume change over the 1989/2006 period has been derived from Special Sensor Microwave/Imager (SSM/I) radiometric measurements for all land surfaces above 50°N, except Greenland. The mean annual snow volumes over the whole study domain, Eurasia and North America are respectively equal to 3713 km^3, 2272 km^3 and 1441 km^3, for the Pan Arctic regions, over this 18-year time period. While the snow volume exhibits a statistically significant negative trend (-9.7 ± 3.8 $km^3.year^{-1}$, p-value=0.02) over North America, it presents a positive, but not statistically significant trend (11.3 ± 9.3 $km^3.year^{-1}$, p-value=0.25) over Eurasia. These opposite variations can be related to different regional climatic conditions over these two regions: over Eurasia, snow depth is mainly influenced by the Arctic Oscillation (AO) and the Atlantic Multidecadal Oscillation (AMO) - correlation coefficient = 0.68 between the SSM/I-derived snow volume and a linear combination of AO and AMO indices, whereas over North America snow depth is mainly influenced by the Pacific North American (PNA) pattern and the AMO - correlation coefficient = 0.75 for a linear combination of the PNA and AMO indices. This study confirms that snow volume is a key driver of the sea level seasonal cycle, but net snow volume trend for the Pan Arctic regions indicates a negligible and not statistically significant contribution to sea level rise (-0.004 ± 0.009 $mm.year^{-1}$, p-value=0.88 once converted into sea level).

Keywords: SSM/I; snow volume; high latitude; climate indices; sea level

1. Introduction

High latitude regions are the most affected by current climate change (e. g. Trenberth et al., 2007). Different components of the Arctic hydrological cycle have experienced important modifications since the beginning of the 20th century. For example river discharge has significantly increased (Stocker and Raible, 2005), snow extent is decreasing (Déry and Brown, 2007; Brown et al., 2010) and the annual duration of the period with unfrozen soil conditions has increased (Groisman et al., 2006). Snow volume is a key variable to understand the evolution of the high latitude hydrological cycle. High latitude rivers discharge is mainly driven by the accumulated snow volume and the timing of its melting, leading to extremely important floods in spring (Yang et al., 2003). So, snow cover extent and depth are among the Essential Climate Variables (ECV) of the Global Climate Observing System (GCOS; Sessa and Dolman, 2008) and observations of their temporal evolution are of critical importance. Few *in situ* snow observations are available at high latitude, thus providing limited information on global and regional snow depth fields (Brown, 2000). Remote sensing techniques complement the *in situ* data, but most analyses focused on snow extent change (see Trenberth et al., 2007 for a review), which only partially characterize snow variability. So far, interannual to multidecadal changes in snow volume have been mainly estimated using hydrological model outputs (e.g. Milly et al., 2003). In this study, we use satellite-based microwave observations to derive and analyze high latitude snow volume changes over 1989/2006. Correlations between snow volume and climate indices have been investigated and the Arctic snow contribution to the global mean sea level variation has been estimated.

2. Data analysis

Snow volume used in this study has been computed from Special Sensor Microwave/Imager (SSM/I) data. SSM/I measures the Earth brightness temperature for different microwave frequencies in both horizontal and vertical polarizations (19.35 GHz, 37 GHz, 85.5 GHz and 22.235 GHz). Since July 1987, this instrument has been operating on board the operational Defense Meteorological Satellite Program satellite series. Daily SSM/I data, mapped to the Equal Area SSM/I Earth Grid projection with a 25×25 km^2 resolution, are provided by the National Snow and Ice Data Center (Armstrong et al., 1994). A dynamic algorithm that takes into account the temporal evolution of the snow grain size, developed by Mognard and Josberger (2002), has been used to retrieve snow depth from SSM/I measurements. This algorithm has been first developed for the U.S. Northern Great Plains, then amended by Grippa et al. (2004) and applied over Western Siberia. Recently, a multi-year (1988/1995) averaged snow depth field computed using this algorithm has been validated over Siberia (Boone et al., 2006) and the whole high latitude regions, Greenland excluded (Biancamaria et al., 2008). Interannual variability of these data has been validated over the Ob river basin, in Western Siberia, by comparison with discharge measurements at the estuary (Grippa et al., 2005). The latter study found a significant correlation between the snowmelt date and the discharge in May (correlation coefficient = -0.92) and between the winter snow depth and the discharge in June (correlation coefficient = 0.61).

The inputs for this algorithm are the difference between 19.35 GHz and 37 GHz brightness temperature in horizontal polarization from SSMI, the air/snow interface temperatures from the National Centers for Environmental Prediction global (NCEP) reanalysis (Kalnay et al., 1996) and the snow/ground interface temperatures modeled by the "Interaction between Soil-Biosphere-Atmosphere" (ISBA) scheme forced by the Global Soil Wetness Project-Phase2 P3 precipitation field (Boone et al., 2006). For the present study, we consider all continental surfaces above 50°N, Greenland excluded, composed of two subregions: Eurasia (0°E<longitude<191°E) and North America (191°E<longitude<360°E). Regions below 50°N have not been taken into account as the snowpack is highly variable spatially and of low amplitude, hence difficult to observe with a 25x25 km^2 spatial resolution. According to the snow climatology over North America from Brown et al. (2003), between December and March, 80% of the total North American snow volume is found above 50°N.

This study focuses on monthly and yearly-averaged total snow volume (sum of all non-zero snow depth pixels multiplied by the pixel area). Yearly averages are centered on winter months (i.e. the yearly average for year n corresponds to the temporal average from October year n-1 to September year n).

Snow volume derived from SSM/I measurements for January, and temporally averaged over 1989/2006, has been compared to the 1979/1996 climatology for North America from Brown et al. (2003) and to the global climatology from U.S. Air Force/Environmental Technical Applications Center (USAF/ETAC) (Foster and Davy, 1988). The correlation coefficient between snow depth from SSM/I and Brown et al. (2003) is 0.36. However most of the differences between the two datasets are found over regions covered with tundra, according to the snow classification from Liston and Sturm, 1998). For tundra-covered regions (42% of North America), the correlation coefficient is equal to 0.20, whereas over the remaining of North America the correlation coefficient is equal to 0.60 (the tundra covers 42% of North America). This result is consistent with the previous study by Biancamaria et al. (2008), which found that the dynamic algorithm does not perform well over the Northern part of the continent (where the tundra is located) due to the presence of numerous lakes. The SSM/I data over these regions need to be processed using a specific algorithm, such as the one developed by Derksen et al. (2010), to take into account the specificity of snow emissivity over lakes. Yet, this still remains an open issue, which requires further investigations since, the *in situ* snow gauges, used by Brown et al. (2003) to compute a climatology by interpolation are very scarce above 50°N, especially for the Northern part of the continent. snow depth from SSM/I correlates better with the USAF/ETAC climatology (correlation coefficient equals to 0.62 over the whole study domain, 0.67 over Eurasia and 0.52 over North America), These correlation coefficients are highly significant, as their p-values (i.e. the probability to obtain these coefficients by random chance, whereas the variables are uncorrelated) are extremely small (lower than 0.001). The snow depth retrieved from SSM/I measurements are not directly compared to *in situ* measurements as the spatial resolution of SSM/I is too coarse to be compared to local measurements, and high latitude networks of *in situ* snow depth measurements are not dense enough to allow an estimation of the mean snow depth over a 25x25 km^2 area. Based on a statistical analysis over the U.S. Northern Great Plains, Chang et al. (2005) showed that error between one single *in situ* measurement and the mean snow depth over a 1°x1° region can be up to 20 cm (for a range of snow depth values between 1.5 cm and 45.4 cm).

The temporal variability of the SSM/I-derived snow volume is analyzed in the next section. It agrees well with previous published studies, giving high confidence in the quality of the snow volume time series estimated from SSM/I observations.

3. Snow volume temporal variability

Figure 1 shows the monthly anomalies of snow volume time series averaged over the study area from SSM/I, from an inversion of the Level-2 GFZ Gravity Recovery And Climate Experiment (GRACE) products (Ramillien et al., 2005; Frappart et al., 2006), from the European Centre for Medium-Range Weather Forecasts ReAnalysis (ERA)-interim product (Uppala et al., 2008), and outputs from two Land Surface Models (LSM) used by the Global Land Data Assimilation System (GLDAS) (Rodell et al., 2004): MOSAIC (Koster and

Suarez, 1996) and NOAH 2.7 (Chen et al., 1996), between January 2003 and June 2006. The mass variations measured by GRACE have been converted into snow volume assuming a constant snow volume density of 300 $kg.m^{-3}$. The time variations of the snow volume are dominated by the seasonal cycle. NOAH outputs present a better agreement with GRACE data both in terms of amplitude and timing. Snow volume from SSM/I is in better agreement with MOSAIC for the amplitude and with ERA-interim for the phase. However, all datasets agree well in phase and their amplitudes have the same order of magnitude, except for ERA-interim which seems to overestimate the amplitude. The GRACE land water and snow solutions used in this study, are based on the development of geopotential harmonic coefficients up to a degree 50, which correspond to a spatial resolution of 400 km (see Frappart et al. (in press) for more details about this dataset). This leads to smaller amplitudes and smoothes the temporal time series. Table 1 presents the annual snow volume trends over 2003/2006 computed from SSM/I-based snow depth, from the snow reservoir extracted from GRACE measurements and from the total GRACE signal over the whole study domain, Eurasia and North America. Two trends computed from GRACE data are shown: the first one has been directly computed from the GRACE (snow and total) time series and the second one has been corrected from the Post-Glacial Rebound (PGR) trend estimated by Paulson et al. (2007), available on the GRACE Tellus website (http://grace.jpl.nasa.gov). The uncertainties on PGR trends are supposed to be around 20% (Paulson et al., 2007) and are given in $mm.year^{-1}$ of equivalent water thickness, which have been converted into snow volume trends using a constant snow density of 300 $kg.m^{-3}$. The PGR trend (in equivalent snow volume per year) is equal to 495.6 $km^3.year^{-1}$, 31.2 $km^3.year^{-1}$ and 464.4 $km^3.year^{-1}$ over the whole study domain, Eurasia and North America, respectively. SSM/I and PGR corrected GRACE trends are all negative, as previously observed at basin-scale for the GRACE data by Frappart et al. (in press), yet they are statistically significant only over North America. The differences between SSM/I and GRACE trends are likely caused by the sensitivity due to the small number of years available for the computation, the truncation of the GRACE data (which caused a loss of energy in the short spatial wavelengths) and PGR uncertainty.

Interannual total snow volume time series (seasonal signal removed) from SSM/I has been computed over 1989/2006 for the whole study domain (Figure 2a) and separately for Eurasia (Figure 2b) and for North America (Figure 2c). Table 2 presents the mean, standard deviation and trend (with the p-value) of the SSM/I-based snow volume over 1989/2006. ERA-interim data has not been used because of biases in the background forecast and in the assimilated observations that makes them unreliable for trend estimation (Trenberth et al., 2007). Even if an effort has been undertaken to reduce the biases in ERA-interim (Dee and Uppala, 2009), trends computed with this dataset should still be used with caution. Outputs from GLDAS are not shown, due to the presence of an obvious bias in these datasets between the 1989/1999 and 2000/2006 time periods. For NOAH, the mean snow volume and standard deviation over 1989/1999 are equal to 6239 km^3 and 329 km^3, respectively, whereas over 2000/2006 they are equal to 4760 km^3 and 183 km^3, respectively. Thus, trends computed from these snow depth fields will mainly be the result of this bias.

SSM/I snow volume over Eurasia displays a positive, but not statistically significant, trend of 11.3±9.3 $km^3.year^{-1}$ (p-value=0.25, Figure 2b), while over North America the trend is negative and statistically significant (-9.7±3.8 $km^3.year^{-1}$, p-value=0.02, Figure 2c). Trends have been computed using the generalized linear model regression (Dobson, 1990), and the uncertainty given with each trend corresponds to the standard error on the estimation of the slope from the linear regression algorithm used. These uncertainties are high as snow volume time series have large variability. When the yearly snow volume is averaged over the whole study domain, the trend is positive, remains small, with a very large uncertainty and is not statistically significant (1.5±10.5 $km^3.year^{-1}$, p-value=0.88, Figure 2a). Figure 3 presents the regional distribution of snow depth trends over 1989/2006 (only statistically significant trends, i.e. p-value<0.1, are shown). Over Eurasia, the highest positive trends are found over the Lena basin, the southern part of the Yenisey basin (between 60°N/70°N and 100°E/130°E) and Eastern Europe. Over North America, Quebec, Baffin Island and the Arctic Ocean coast show negative trends, whereas positive trends are found over the Rockies and Southern Alaska. Previous studies interpolated sparse *in situ* measurements to infer temporal evolution of snow cover. Groisman et al. (2006) analyzed 1811 *in situ* observations of the soil condition (classified as frozen or unfrozen) between 1956 and 2004, within 1197 1°x1° grid cells over the former Soviet Union (most of these grid cells containing only one *in situ* station). The *in situ* network used is very sparse above 55°N and East of the Ural Mountains. Groisman et al. (2006) observed a significant increase in the number of days with unfrozen soil conditions between 1956 and 2004. Yet, this increase is most frequently due to a reduction of days with frost and ice on the ground rather than a snow cover retreat. Besides, these modifications tend to diminish during the last decade of the twentieth century. These observations agree with our results (a positive, but not significant, snow volume trend over Eurasia). Bulygina et al. (2009) used 820 *in situ* stations over Russia between 1966 and 2007 to infer snow depth trend maps. They found that snow cover periods tend to be shorter, however the amount of snow fall tends to increase, leading to positive snow depth trends over Eurasia: maximum storage change increased from 0.2 $cm.year^{-1}$ to 0.6/0.8 $cm.year^{-1}$ (with maximum rates in Western Siberia). These trends have the same order of magnitude than trends shown in Figure 3. Based on *in situ* measurements, Kitaev et al. (2005) found a positive snow depth trend (0.09 $cm.year^{-1}$) over Eurasia (for latitudes above 40°N) for February between 1936/2000. This study also showed opposite trends between snow water equivalent in February for 1966/2000 over Eurasia and North America (the trends are equal to 0.743 mm/decade and -1.231 743 mm/decade, respectively). For February of the 1989/2006 time span, SSM/I-based snow depth trends are equal to 0.14 cm.year^{-1} (p-value=0.15) over Eurasia and -0.18 cm.year^{-1} (p-value=0.02) over North America. These results are in agreement with the results found by Kitaev et al. (2005).

Using different data sets (visible and microwave satellite observations, objective analyses of surface snow depth observations, reconstructed snow cover from daily temperature and precipitation, and proxy information derived from thaw dates), Brown et al. (2010) showed that snow cover extent in June and May respectively decreased by 46% and a 14% in the Arctic (latitude>60°N), during the 1967/2008 time period. This reduction is observed over both Eurasia and North America and 56% of snow cover extent variability for June and 49% for May is explained by air temperature. Using a less accurate data set, Déry and Brown (2007) showed that snow cover extent also decreased in Eurasia and North America during winter time for the 1972/2006 time span. However, the observed decline is smaller than during spring. The snow volume variability computed in our study does not seem to be consistent with the trend in snow cover extent observed in these previous studies, especially over Eurasia. Yet, this was expected. In effect, Ge and Gong (2008) showed that, at continental/regional scales, high latitude snow extent and snow depth are largely unrelated.

The decreasing trend of snow volume over North America estimated from SSM/I is in agreement with the previous study from Dyer and Mote (2006). Using interpolated *in situ* measurements during the 1960/2000 time span, they found that snow depth has a decreasing trend in January/February over the time period, which becomes even steeper around March, along with an earlier onset of spring thaw, which could explain the decreasing North American snow volume trend observed in our study.

It is extremely difficult to estimate the implications of the observed decreased in North American snow volume on other snow related parameters, like glaciers mass, and an answer to this issue is far beyond the scope of this paper. For example, very recently, Berthier et al.

(2010) confirmed that Alaskan glaciers are losing mass. However, glaciers mass loss is not only observed in North America, but is widely measured on all continents (Kaser et al., 2006). Therefore, it is hard to assess if there is any relation between the Alaskan glaciers mass loss and the decreasing snow volume in North America, and this issue will require further investigations.

4. Relationship between snow volume and climate indices

To investigate the causes of snow volume variability in North America and Eurasia, yearly mean SSM/I snow volume anomaly has been correlated to climate indices representing the dominant modes of atmospheric and ocean variability. The following climate indices have been considered:

- Arctic Oscillation (AO, leading mode from the Empirical Orthogonal Function analysis of monthly mean height anomalies at 1000-hPa, poleward of 20°N). A positive (negative) AO index corresponds to a lower (higher) than normal atmospheric pressure over the Artcic, which leads to stronger (weaker) westerly winds. Therefore, in positive AO phase , cold Arctic air is maintained in the Northern part of America (Arctic coast and Quebec), while the rest of America, Europe and Asia experiences a warmer then averaged winter, with more precipitation in Northern Europe. On the contrary, in negative AO phase, cold Arctic air reaches lower latitude (South Canada, US, Asia and Europe), whereas the Northern parts of America is warmer than during the positive AO phase (Thompson and Wallace, 1998).
- Atlantic Multidecadal Oscillation (AMO, North Atlantic mean sea surface temperature anomaly north of the equator). AMO corresponds to cycles of warming and cooling of the North Atlantic Ocean with a period comprised between 50 and 80 years. This cycle affects the North Atlantic branch of the thermohaline circulation and therefore the whole oceanic system

(Kerr, 2000). A positive (negative) phase of the AMO leads to more (less) summer precipitations in Northern Europe and Alaska and less (more) summer precipitations in the U.S. and South Canada (Enfield et al., 2001). Knight et al. (2006) show, using a climate model, that positive AMO phase tends to strengthen broad cyclonic pressure anomalies over the Atlantic and Europe in winter, therefore increasing precipitations on these regions. During the time span of the study (1989/2006), the AMO has shifted from a negative to a positive phase around 1995.

- Pacific Decadal Oscillation (PDO, leading principal component of monthly sea surface temperatures in the North Pacific, poleward of 20°N). PDO is an El Niño-like pattern characteristic the North Pacific climate variability with interannual to interdecadal fluctuations. PDO influences mainly North America climate during winter time and is positively correlated with precipitation along the coasts and central Gulf of Alaska and negatively correlated over much of the interior of North America (Mantua et al., 1997).
- Pacific North American pattern (PNA, second component of the Northern Hemisphere extra tropical sea level pressure anomalies). During positive (negative) phase of the PNA, geopotential height anomalies are positive (negative) along the West coast of North America and negative (positive) in the mid-Pacific and Eastern US. Therefore, negative PNA phase is characterized by a strong East Asian jet stream, which is blocked during positive PNA phase. The spatial scale of the PNA pattern is at its most extent during winter (Wallace and Gutzler, 1981).

Data have been computed by the National Oceanic and Atmospheric Administration (NOAA)/Climate Prediction Center (CPC), the NOAA/Earth System Research Laboratory (ESRL) and the Joint Institute for the Study of the Atmosphere and Ocean (JISAO)/University of Washington (UW), and have been downloaded from http://ioc3.unesco.org/oopc/state_of_the_ocean/atm. Each index has been averaged from January through March for each year.

Figure 4 presents annual snow volume time series over Eurasia and North America along with the January to March average of the climate indices presented above. As snow volumes and the indices do not have the same units and range of variations, all time series shown in Figure 4 have been normalized and centered. On each plot, the gray horizontal line corresponds to the zero in the original climate index time series. Table 3 gives the correlation coefficients between the climate indices and the annual snow volumes over North America and Eurasia. The AO index is relatively well correlated with snow volume over North America (correlation=0.51 and p-value=0.03, Figure 4b) and anti-correlated with snow volume over Eurasia (correlation=-0.57 and p-value=0.01, Figure 4a), thus the climatic conditions represented by the AO index (which is the dominant mode of interannual variability in North Hemisphere) play a significant and opposite role over the two continents. It is worth mentioning that SSM/I snow volume over Eurasia and North America are not correlated (correlation=-0.07 and p-value=0.80). AMO and PNA are anti-correlated with snow volume over North America (correlation=-0.59 with p-value=0.01 and correlation=-0.66 with p-value=0.003, respectively) and not, or only weakly, correlated with snow volume over Eurasia (correlation=0.04 with p-value=0.88 and correlation=0.30 with p-value=0.22, respectively). On the contrary, PDO is more strongly linked with snow volume over Eurasia (correlation=0.49 with p-value=0.04) than over North America (correlation=-0.18 with p-value=0.47). Figure 5 presents snow depth linear regression maps based on each climate index (i.e. the correlation coefficient between snow depth and the climate index multiplied by the snow depth standard deviation for each pixel), which clearly show the locations where snow depth co-varies with each climate index. On these maps, regression coefficients are presented only for pixels which have a statistically significant (p-value<0.1) correlation coefficient. Regression map between snow depth and AO index (Figure 5a) clearly shows the opposite impact of AO index over snow depth between North American Arctic coast and the Eastern part of Siberia (with positive regression coefficients) and middle Siberia and Eastern Europe (with negative regression coefficients). There are few statistically significant regression coefficients between snow depth and AMO index over Eurasia (Figure 5b), some negative regression coefficients over Quebec and North American Arctic coast and some positive coefficients over the Rockies. Snow depth weakly co-varies with PDO index over North America (Figure 5c), contrarily to Southern middle Siberia and Northeastern Europe, where regression coefficients are positive. Finally, regression coefficients between snow depth and PNA index (Figure 5d) show that PNA is linked with snow depth especially in central North America (negative coefficients), in the Rockies (positive coefficients) and in Southern middle Siberia (positive coefficients). From these results, it seems that AO is the only mode affecting significantly snow volumes over both Eurasia and North America and could explain the different behavior of snow volume over these two continents.

Previous studies (Cohen et al., 2007; Orsolini and Kvamstø, 2009) have shown that high snow cover in late autumn over Eurasia can create upward propagating planetary wave pulses in winter, which weaken the polar vortex and therefore lead to negative AO in late winter, explaining a negative correlation between snow cover extent and AO index. The same process also explains the negative correlation between snow volume over Eurasia and winter AO index observed in our study.

Ge and Gong (2009) compared monthly AO, NAO (North Atlantic Oscillation, commonly seen as a regional manifestation of AO), PDO and PNA indices with monthly *in situ* interpolated snow depth over North America during the 1956/2000 time span. They found that snow depth has weak correlation with monthly AO and NAO indices, but strong anti-correlation with monthly PDO and PNA indices for the winter months (December to April).

However, for PDO, only correlation coefficients for February and March are significant at 90% confidence level (for PNA all the correlations during all winter months are above the 90% confidence level). Our results seem to differ partially, as we found that snow volume significantly correlates with AO, significantly anti-correlates with PNA and has no significant linear relationship with PDO over North America. However, it should be noted that Ge and Gong (2009) studied a wider domain (with latitudes below 35°N) and found the highest relations between snow depth and PDO/PNA over interior central-western North America, which expands far below 50°N (the Southern limit of our study domain). Ghatak et al. (2010) used the same North American *in situ*-based snow depth field than Ge and Gong (2009) and found that globally snow depths correlate negatively with both winter NAO and PNA. Yet, their study domain includes the whole North American continent. If only the latitudes above 50°N are considered (Figure 4 and 6 in Ghatak et al., 2010), they showed that snow depth correlates positively with NAO and negatively with PNA, as found in our study (Table 3). Their explanation of these correlations is the following: positive phase of winter NAO leads to higher air temperature anomalies over eastern North America, reducing snow volume; positive phase of the winter PNA leads to stronger East Asian jet stream and thus more snowfall in Northwest America but to less snowfall in Northeast America and near the Arctic coast (which is in agreement with the regression map between snow depth and PNA, Figure 5d).

To better examine inter-annual co-variability between snow volume and climate indices, the linear trend in all time series has been removed and the corresponding correlation coefficients have been computed (Table 3). Over Eurasia, the most statistically significant correlations are still obtained with the AO (correlation=-0.51 with p-value=0.03) and PDO (correlation=0.41 with p-value=0.09) indices. Over North America, the only statistically significant correlation is obtained with PNA index (correlation=-0.58 with p-value=0.01), which means that North American snow volume linear trend could be related to the AO and AMO indices (probably due to the shift from a negative to a positive AMO around 1995), whereas snow volume inter-annual variability is more linked with the PNA pattern.

The correlation coefficients between yearly mean snow volume anomaly and all possible linear combinations of two different climate indices have also been computed. For Eurasia, the best correlation coefficient (0.68, p-value=0.002) is obtained for a linear combination between AO and AMO (-156.AO-611.AMO, blue curve in Figure 2b), whereas for North America the best correlation coefficient (0.75, p-value<0.01) is obtained for a linear combination between PNA and AMO (-235.AMO-92.PNA, blue curve in Figure 2c). AO and PNA, when combined with AMO, influence respectively the most Eurasia and North America snow volume and represent regional atmospheric processes influencing the two continents. If the trend is removed from both climate indices and snow volume, the best correlation coefficient is still obtained with a linear combination of AO and AMO indices over Eurasia (-136.AO-940.AMO, correlation=0.68 and p-value=0.002). Surprisingly, linear combination of AO and PDO indices, which individually gives respectively the first (-0.51) and second (0.41) best correlations with snow volume over Eurasia, only corresponds to the second best correlation between a linear combination of two climate indices and snow volume (-96.AO+76.PDO, correlation=0.58 and p-value=0.01). Over North America, the best correlation is obtained with a linear combination of PDO and PNA indices (37.PDO-114.PNA, correlation=0.66 and p-value=0.003), however the second best correlation is obtained with AMO and PNA indices (-165.AMO-87.PNA, correlation=0.61 and p-value=0.007).

5. Snow and sea level

High latitude snow has a large impact on river discharge and thus is the main source of fresh water input to the Arctic Ocean. Snow volume change (V_{snow}) presented in the previous sections can be used to estimate the snow contribution to the global mean sea level (SLV_{snow}), using equation (1).

$$SLV_{snow} = -\frac{\rho_{snow}}{\rho_{water} \cdot A_{ocean}} \cdot V_{snow} \qquad (1)$$

where ρ_{snow}=300 kg.m^{-3} (snow density), ρ_{water}=1000 kg.m^{-3} (liquid water density) and A_{ocean}=3.6x10^{8} km^{2} (total oceanic domain).

Over 1989/2006, the snow volume trend from SSM/I converted into equivalent sea level is very small (-0.0013±0.0087 mm.yr^{-1}) and not statistically significant. The snow volume trend over the altimetry time span (1993/2006) amounts to -17.0±15.1 km^{3}.year^{-1} (p-value=0.28), which yield small positive contributions to sea level of 0.014±0.013 mm.yr^{-1}. As this trend is not statistically significant and is negligible compared to the global mean sea level trend (of 3.3±0.4 mm.yr^{-1} over the satellite altimetry period 1993/2009; Cazenave and Llovel, 2010), it is obvious that high latitude snow does not play any role in the global mean sea level rise observed from satellite altimetry.

However, Arctic snow is a key component of the mean sea level seasonal cycle. To investigate this relationship, snow volume change has been compared to global mean sea level time series over 2002/2006 from Topex/Poseidon and Jason 1 computed by Collecte Localisation Satellite (CLS), available on the AVISO website (www.aviso.oceanobs.com). The mean sea level data have been corrected for steric effects (mainly thermal expansion of ocean waters) using the methodology developed by Llovel et al. (2010) and based on Argo data (Guinehut et al., 2009). Mean and trend have been removed from this corrected sea level and the seasonal cycle (i.e. the sinusoid with a 365.25 day period which best fits the time series) has been least square adjusted. The sea level seasonal cycle has a maximum amplitude of 6.2 mm which occurs around 15 October. Snow volume converted into sea level (mean and trend removed) has a seasonal cycle with 4.1 mm maximum amplitude around 10 August. Its amplitude is smaller, but has the same order of magnitude than the global mean sea level seasonal cycle, yet breaks earlier. This phase lag could be due to the time taken by water from snow melt to be routed to the ocean by the river network. It could also be explained if water stored in other reservoirs like ground water and water vapor in the atmosphere is taken into account. To test this hypothesis, the seasonal cycle of the ground water has been approximated by a sinusoid with amplitude of 3 mm (in sea level equivalent) and a yearly maximum at the beginning of September (Cazenave et al., 2000). Similarly, the atmospheric water vapor has been approximated by a sinusoid with amplitude of 2 mm and a yearly maximum at the beginning of December (Cazenave et al., 2000). The sum of these three contributors (snow, ground water and water vapor) has an amplitude equal to 6.9 mm, which is very close to the global mean sea level seasonal cycle amplitude with a reduced phase lag (the maximum is around mid-September). This is a surprisingly good result given the large approximation used and clearly shows that Arctic snow variability is one of the main contributors to the global mean sea level seasonal cycle, as previously shown from model outputs by Chen et al. (1998), Minster et al. (1999), Cazenave et al. (2000) and Milly et al. (2003).

6. Conclusions and perspectives

From passive microwave data acquired between 1989 and 2006, it has been possible to estimate the high latitude snow volume variability. Over Eurasia, the mean annual snow volume trend is positive (11.3 ± 9.3 km^3.year^{-1}), yet not statistically significant. Over North

America the snow volume trend is equal to -9.7±3.8 $km^3.year^{-1}$ and is statistically significant. This difference between the two continents could be due to AO which correlates with North American snow volume (correlation = 0.51) and anti-correlates with Eurasian snow volume (correlation = -0.57). These differences are also linked with regional climatic conditions as snow volume anomaly over North America better (anti-)correlates with the PNA index (correlation=-0.66), and AMO index (correlation=-0.59). However, the correlation between AMO and North American snow volume is mainly due to the trend and not to the interannual variability. Moreover, snow volume over Eurasia correlates well with a linear combination of the AO and AMO indices (correlation = 0.68), whereas over North America it correlates with a linear combination of the PNA and AMO indices (correlation = 0.75).

Finally, this study shows that high latitude snow volume does not contribute to the global mean sea level trend observed by satellite altimetry, but is a main component of the global mean sea level seasonal cycle.

In the future, it will be interesting to compare the snow volume trends observed in this study and trends from other hydrologic parameters in order to better understand the interaction between snow and the whole North Hemisphere high latitude hydrological cycle.

Acknowledgments

The NSIDC is greatly thanked for processing and freely distributing SSM/I data.

The GLDAS data used in this study were acquired as part of the mission of NASA's Earth Science Division and archived and distributed by the Goddard Earth Sciences (GES) Data and Information Services Center (DISC). The Authors are thankful to J.-P. Vergnes for downloading and post-processing GLDAS data.

ECMWF ERA-Interim data used in this study have been obtained from the ECMWF data server.

The NOAA/CPC, NOAA/ESRL and JISAO/UW are acknowledged for letting the time series of the climate indices used in this study freely available to the community. The authors are particularly grateful to two anonymous reviewers for their constructive comments and suggestions, which significantly improved the quality of the manuscript. Three of the authors are supported by a CNES/Noveltis PhD grant (S. Biancamaria), a STAE foundation grant in the framework of the CYMENT project (F. Frappart) and a CNRS/Région Midi-Pyrénées PhD grant (W. Llovel).

References

Armstrong, R.L., Knowles, K.W., Brodzik, M.J., Hardman, M.A., 1994 (updated 2007). DMSP SSM/I Pathfinder daily EASE-Grid brightness temperatures 1988-2006. National Snow and Ice Data Center, Digital media, Boulder, Colorado USA.

Berthier, E., Schiefer, E., Clarke, G.K.C., Menounos, B., Rémy, F., 2010. Contribution of Alaskan glaciers to sea-level rise derived from satellite imagery. Nat. Geosci., 3, 92-95.

Biancamaria, S., Mognard, N.M., Boone, A., Grippa, M., Josberger, E.G., 2008. A satellite snow depth multi-year average derived from SSM/I for the high latitude regions. Remote Sens. Environ., 112, 2557-2568.

Boone, A., Mognard, N.M., Decharme, B., Douville, H., Grippa, M., Kerrigan, K., 2006. The impact of simulated soil temperatures on the estimation of snow depth over Siberia from SSM/I compared to a multi-model multi-year average. Remote Sens. Environ., 101, 482-494.

Brown, R.D., 2000. Northern Hemisphere snow cover variability and change, 1915-97. J. Clim., 13, 2339-2355.

Brown, R.D., Brasnett, B., Robinson, D., 2003. Gridded North American monthly snow depth and snow water equivalent for GCM evaluation. Atmos. Ocean., 41, 1-14.

Brown, R.D., Derksen, C., Wang, L., 2010. A multi-data set analysis of variability and change in Arctic spring snow cover extent, 1967-2008. J. Geophys. Res., 115, D16111.

Bulygina, O.N., Razuvaev, V.N., Korshunova, N.N., 2009. Changes in snow cover over Northern Eurasia in the last few decades. Environ. Res. Lett., 4, doi:10.1088/1748-9326/4/4/045026.

Cazenave, A., Remy, F., Dominh, K., Douville, H., 2000. Global ocean mass variation, continental hydrology and the mass balance of Antarctica ice sheet at seasonal time scale. Geophys. Res. Lett., 27, 3755-3758.

Cazenave, A., Llovel, W., 2010. Contemporary sea level rise. Annu. Rev. Mar. Sci., 2, 145-173, doi:10.1146/annurev-marine-120308-081105.

Chang, A.T.C., Kelly, R.E.J., Josberger, E.G., Armstrong, R.L., Foster, J.L., Mognard, N.M., 2005. Analysis of ground-measured and passive microwave derived snow depth variations in mid-winter across the Northern Great Plains. J. Hydrometeorol., 6, 20-33.

Chen, F., Mitchell, K., Schaake, J., Xue, Y., Pan, H.-L., Koren, V., Duan, Q.Y., Ek, M., Betts, A., 1996. Modeling of land-surface evaporation by four schemes and comparison with FIFE observations. J. Geophys. Res., 101, D3, 7251-7268.

Chen, J.L., Wilson, C.R., Chambers, D.P., Nerem, R.S., Tapley, B.D., 1998. Seasonal global water mass budget and mean sea level variations. Geophys. Res. Lett., 25, 3555-3558.

Cohen, J., Barlow, M., Kushner, P.J., Saito, K., 2007. Stratopshere-Troposphere coupling and links with Eurasian land surface variability. J. Clim., 20, 5335-5343.

Dee, D.P., Uppala, S., 2009. Variational bias correction of satellite radiance data in the ERA-interim reanalysis. Q. J. R. Meteorol. Soc., 135, 1830-1841.

Derksen, C., Toose, P., Rees, A., Wang, L., English, M., Walker, A., Sturm, M., 2010. Development of a tundra-specific snow water equivalent retrieval algorithm for satellite passive microwave data. Remote Sens. Environ., 114, 1699-1709.

Déry, S.J., Brown, R.D., 2007. Recent Northern Hemisphere snow cover extent trends and implications for the snow-albedo feedback. Geophys. Res. Lett., 34, L22504.

Dobson, A.J., 1990. An introduction to generalized linear models. CRC Press, New York.

Dyer, J.L., Mote, T.L., 2006. Spatial variability and trends in snow depth over North America. Geophys. Res. Lett., 33, L16503.

Enfield, D.B., Mestas-Nunez, A.M., Trimble, P.J., 2001. The Atlantic Multidecadal Oscillation and its relationship to rainfall and river flows in the continental U.S.. Geophys. Res. Lett., 28, 2077-2080.

Foster, D.J., Davy, R.D., 1988. Global snow depth multi-year average. USAFETAC/TN-88/006, Illinois: Scott Air Force Base, 48 pp.

Frappart, F., Ramillien, G., Biancamaria, S., Mognard, N.M., Cazenave, A., 2006. Evolution of high-latitude snow mass derived from the GRACE gravimetry mission (2002-2004). Geophys. Res. Lett., 33, L02501.

Frappart, F., Ramillien, G., Famiglietti, J.S., in press. Water balance of the Arctic drainage system using GRACE gravimetry products. Int. J. Remote Sens., doi: 10.1080/01431160903474954.

Ghatak, D., Gong, G., Frei, A., 2010. North American temperature, snowfall, and snow-depth response to winter climate modes. J. Clim., 23, 2320-2332.

Ge, Y., Gong, G., 2008. Observed inconsistencies between snow extent and snow depth variability at regional/continental scales. J. Clim., 21, 1066-1082.

Ge, Y., Gong, G., 2009. North American snow depth and climate teleconnection patterns. J. Clim., 22, 217-233.

Grippa, M., Mognard, N.M., Le Toan, T., Josberger, E.G., 2004. Siberia snow depth multi-year average derived from SSM/I data using a combined dynamic and static algorithm. Remote Sens. Environ., 93, 30-41.

Grippa, M., Mognard, N.M., Le Toan, T., 2005. Comparison between the interannual variability of snow parameters derived from SSM/I and the Ob river discharge. Remote Sens. Environ., 98, 35-44.

Groisman, P.Y., Knight, R.W., Razuvaev, V.N., Bulygina, O.N., Karl, T.R., 2006. State of the ground: climatology and changes during the past 69 years over Northern Eurasia for a rarely used measure of snow cover and frozen land. J. Clim., 19, 4933-4955.

Guinehut, S., Coatanoan, C., Dhomps, A.-L., Le Traon, P.-Y., Larnicol, G., 2009. On the use of satellite altimeter data in Argo quality control. J. Atmos. Oceanic Technol., 46, 85-98.

Kalnay, E., Kanamitsu, M., Kistler, R., Collins, W., Deaven, D., Gandin, L., Iredell, M., Saha, S., White, G., Woollen, J., Zhu, Y., Chelliah, M., Ebisuzaki, W., Higgins, W., Janowiak, J., Mo, K.C., Ropelewski, C., Wang, J., Leetmaa, A., Reynolds, R., Jenne, R., Joseph D., 1996. The NCEP/NCAR 40-year reanalysis project. Bull. Am. Meteorol. Soc., 77, 437-471.

Kaser, G., Cogley, J.G., Dyurgerov, M.B., Meier, M.F., Ohmura, A., 2006. Mass balance of glaciers and ice caps: Consensus estimates for 1961-2004. Geophys. Res. Lett., 33, L19501.

Kerr, R.A., 2000. A North Atlantic climate pacemaker for the centuries. Science, 288, 1984-1986.

Kitaev, L., Førland, E., Razuvaev, V., Tveito, O.E., Krueger, O., 2005. Distribution of snow cover over Northern Eurasia. Nord. Hydrol., 36, 311-319.

Knight, J.R., Folland, C.K., Scaife, A.A., 2006. Climate impacts of the Atlantic Multidecadal Oscillation. Geophys. Res. Lett., 33, L17706.

Koster, R.D., Suarez, M. J., 1996. Energy and water balance calculations in the Mosaic LSM, NASA Tech. Memo. 104606, 9, 76 pp.

Liston, G.E., Sturm, M., 1998. Global Seasonal Snow Classification System. National Snow and Ice Data Center Digital media, Boulder, CO, USA.

Llovel, W., Guinehut, S., Cazenave, A., 2010. Regional and interannual variability in sea level over 2002-2009 based on satellite altimetry, Argo float data and GRACE ocean mass. Ocean Dynam., 60, 1193-1204, doi:10.1007/s10236-010-0324-0.

Mantua, N.J., Hare, S.R., Zhang, Y., Wallace, J.M., Francis, R.C., 1997. A Pacific interdecadal climate oscillation with impacts on salmon production. Bull. Am. Meteorol. Soc., 78, 1069-1079.

Milly, P.C.D., Cazenave, A., Gennero, M.-C., 2003. Contribution of climate-driven change in continental water storage to recent sea-level rise. Proc. Natl. Acad. Sci. U.S.A., 100, 13158-13161.

Minster, J.F., Cazenave, A., Serafini, Y.V., Mercier, F., Gennero, M.-C., Rogel, P., 1999. Annual cycle in mean sea level from Topex-Poseidon and ERS-1: inference on the global hydrological cycle. Global Planet. Change, 20, 57-66.

Mognard, N.M., Josberger, E.G., 2002. Northern Great Plains 1996/97 seasonal evolution of snowpack parameters from satellite passive-microwave measurements. Ann. Glaciol., 34, 15-23.

Orsolini, Y.J., Kvamstø, N.G., 2009. Role of Eurasian snow cover in wintertime circulation: Decadal simulations forced with satellite observations. J. Geophys. Res., 114, D19108.

Paulson, A., Zhong, S., Wahr, J., 2007. Inference of mantle viscosity from GRACE and relative sea level data. Geophys. J. Int., 171, 497-508.

Ramillien, G., Frappart, F., Cazenave, A., Güntner, A., 2005. Time variations of the land water storage from an inversion of 2 years of GRACE geoids. Earth Planet. Sci. Lett., 235, 283-301.

Rodell, M., Houser, P.R., Jambor, U., Gottschalck, J., Mitchell, K., Meng, C.-J., Arsenault, K., Cosgrove, B., Radakovich, J., Bosilovich, M., Entin, J.K., Walker, J.P., Lohmann, D., Toll, D., 2004. The global land data assimilation system. Bull. Am. Meteorol. Soc., 85, 381-394.

Sessa, R., Dolman, H., 2008. Terrestrial Essential Climate Variables, GTOS n°52, biennal report supplement, 40 pp., FAO, Rome, Italy.

Stocker, T.F., Raible, C.C., 2005. Water cycle shifts gear. Nature, 434, 830-833.

Thompson, D.W.J., Wallace, J.M., 1998. The Arctic Oscillation signature in the wintertime geopotential height and temperature fields. Geophys. Res. Lett., 25, 1297-1300

Trenberth, K.E., Jones, P.D., Ambenje, P., Bojariu, R., Easterling, D., Klein Tank, A., Parker, D., Rahimzadeh, F., Renwick, J. A., Rusticucci, M., Soden, B., Zhai, P., 2007. Observations: Surface and Atmospheric Climate Change. In Climate change 2007: the physical science basis. Contribution of Working Group I to the Fourth Assessment report of the Intergouvernmental Panel on Climate Change, edited by S. Solomon et al., pp. 235-336 and SM.3-8, Cambridge Univ. Press, Cambridge, U. K.

Uppala, S., Dee, D., Kobayashi, S., Berrisford, P., Simmons, A., 2008. Towards a climate data assimilation system: status update of ERA-Interim. ECMWF newsletter, 115, 12-18.

Wallace, J.M., Gutzler, D.S., 1981. Teleconnections in the geopotential height field during the Northern Hemisphere winter. Mon. Wea. Rev., 109, 784-812.

Yang, D., Robinson, D., Zao, Y., Estilow, T., Ye, B., 2003. Streamflow response to seasonal snow cover extent changes in large Siberian watersheds. J. Geophys. Res., 108, 4578, doi: 10.1029/2002JD003419.

Table captions:

Table 1. Annual snow volume trends over 2003/2006 computed from SSM/I snow volume, snow reservoir extracted from GRACE and from the total GRACE signal over the whole study domain, Eurasia and North America

Table 2. Mean, standard deviation and trend of annual snow volume retrieved from SSM/I measurements during 1989/2006 period over the whole study domain, Eurasia and North America; p-values (p) for trends are indicated in parentheses.

Table 3. Correlation coefficients from January to March average of the climate indices (AO, AMO, PDO and PNA) and annual snow volumes over North America and Eurasia (the p-value of each correlation is indicated in parentheses). The correlations are computed both with and without trend in the time series of both snow volume and climate indices.

Figure captions:

Figure 1. Total snow volume for all continental surfaces above 50°N (Greenland excluded) estimated from SSM/I (red curve), GRACE (orange curve), ERA-interim reanalysis (black curve), MOSAIC model (green curve) and NOAH model (blue curve).

Figure 2. Annual snow volume from SSM/I data (solid red curve) over the whole study domain (a.), over Eurasia (b.) and over North America (c.). On each plot the black line corresponds to the linear trend and the blue curve corresponds to the linear combination of

two climate indices (January to March average) which best correlates with SSM/I snow volume (the mean value of the SSM/I snow volume over the 1989/2006 period has been added to the linear combination).

Figure 3. Map of the annual snow depth trends over the 1989/2006 time span. Only statistically significant trends are shown (i.e. trends with p-value < 0.1).

Figure 4. Annual snow volume over Eurasia (red curves in a., b., c., d.) and over North America (red curves in e., f., g., h.) and January to March average of AO (blue cruves in a., e.), AMO (blue cruves in b., f.), PDO (blue cruves in c., g.) and PNA (blue cruves in d., h.) indices versus time. The time series have been normalized and centered to be plotted at the same scale. On each plot, the gray horizontal line corresponds to the zero in the original climate index time series.

Figure 5. Regression maps between annual snow volume and January to March average of AO (a.), AMO (b.), PDO (c.) and PNA (d.) indices for the 1989/2006 time span. On each map are shown pixels with a statistically significant (p-value < 0.1) correlation coefficient between snow volume and the considered climate index.

Tables:

Table 1:

	Annual snow volume trend for 2003/2006 ($km^3.year^{-1}$)				
	SSM/I	GRACE snow no PGR corr.	GRACE snow PGR corr.	GRACE total no PGR corr.	GRACE total PGR corr.
Whole domain	-71.4±83.5 (p=0.48)	46.8±103.4 (p=0.70)	-448.8	179.0±234.3 (p=0.52)	-316.6
Eurasia	-20.0±82.8 (p=0.83)	-91.3±57.5 (p=0.25)	-122.5	-237.2±231.4 (p=0.41)	-268.4
North America	-51.4±9.6 (p=0.03)	138.1±46.2 (p=0.10)	-326.3	416.3±52.0 (p=0.02)	-48.1

Table 2:

	SSM/I annual snow volume		
	Whole domain	Eurasia	North America
1989/2006 mean (km^3)	3713	2272	1441
Std (km^3)	218	189	95
Trend ($km^3.year^{-1}$)	1.5±10.5 (p=0.88)	11.3±9.3 (p=0.25)	-9.7±3.8 (p=0.02)

Table 3 :

		AO	AMO	PDO	PNA
Eurasian snow depth	with trend	-0.57 (p=0.01)	0.04 (p=0.87)	0.49 (p=0.04)	0.30 (p=0.22)
	without trend	-0.51 (p=0.03)	-0.33 (p=0.18)	0.41 (p=0.09)	0.21 (p=0.39)
North American snow depth	with trend	0.51 (p=0.0 3)	-0.59 (p=0.01)	-0.18 (p=0.47)	-0.66 (p=0.003)
	without trend	0.25 (p=0.31)	-0.31 (p=0.20)	0.10 (p=0.71)	-0.58 (p=0.01)

Figures:

Figure 1:

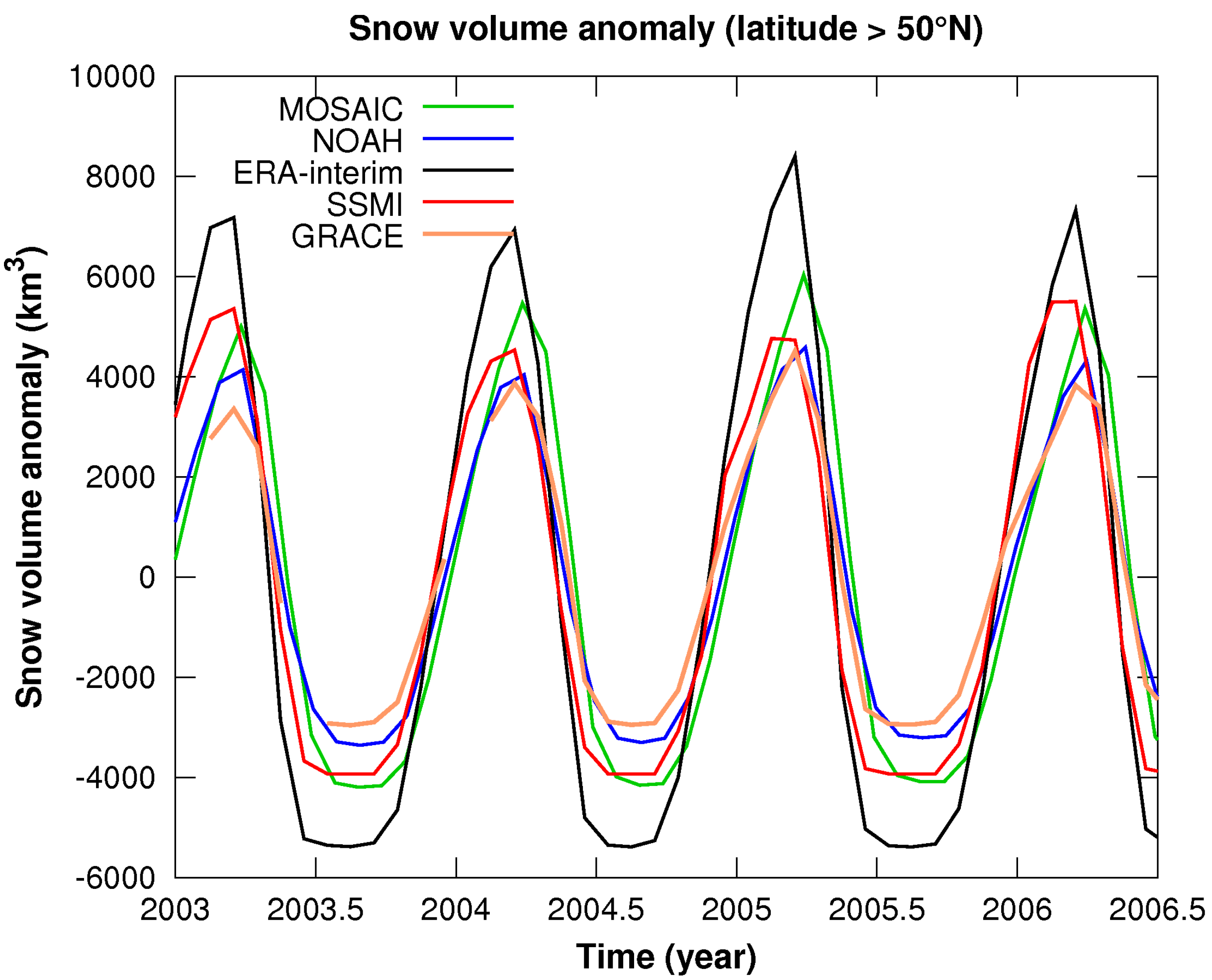

Figure 2:

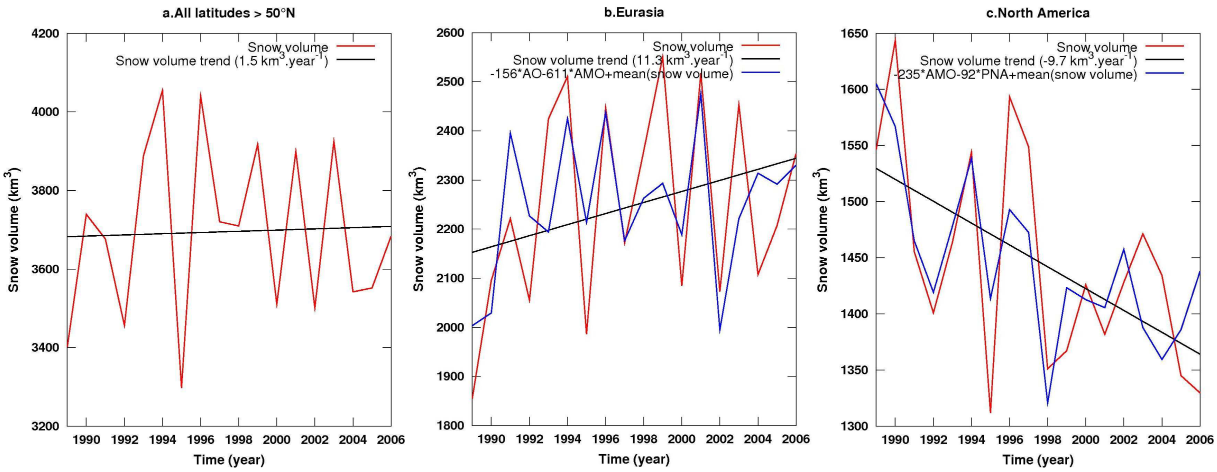
a.All latitudes > 50°N
Snow volume
Snow volume trend (1.5 km3.year-1)
b.Eurasia
Snow volume
Snow volume trend (11.3 km3.year-1)
-156*AO-611*AMO+mean(snow volume)
c.North America
Snow volume
Snow volume trend (-9.7 km3.year-1)
-235*AMO-92*PNA+mean(snow volume)
Snow volume (km3)
Time (year)

Figure 3:

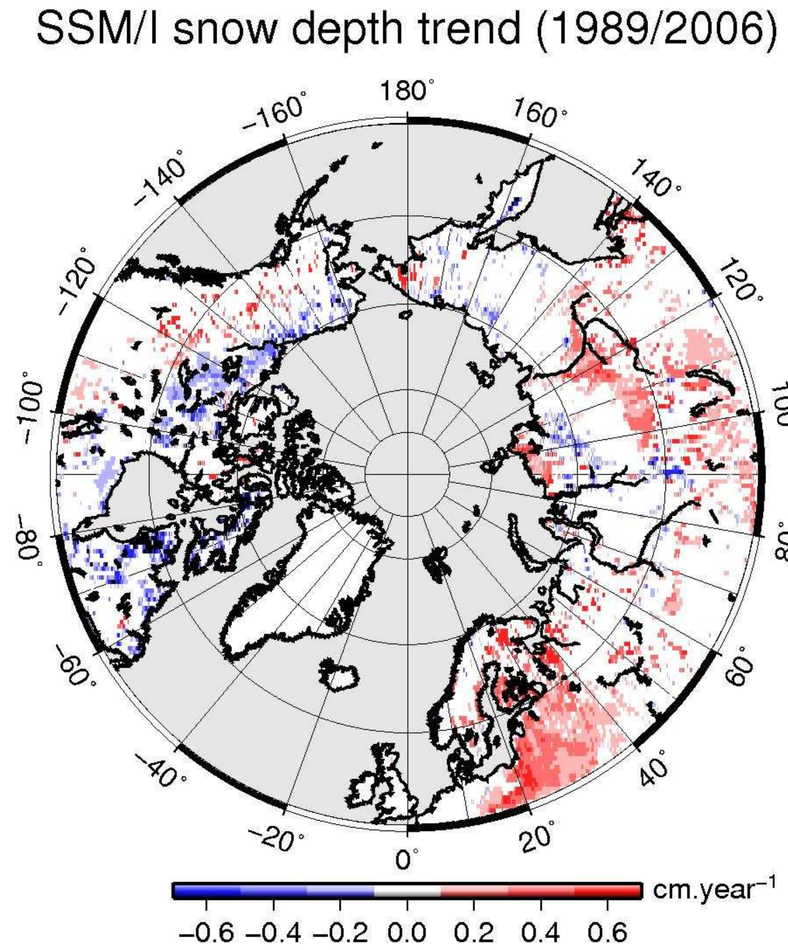

SSM/I snow depth trend (1989/2006)
180°
−160°
160°
−140°
140°
−120°
120°
−100°
100°
−80°
80°
−60°
60°
−40°
40°
−20°
20°
0°
cm.year^{-1}
−0.6 −0.4 −0.2 0.0 0.2 0.4 0.6

Figure 4 :

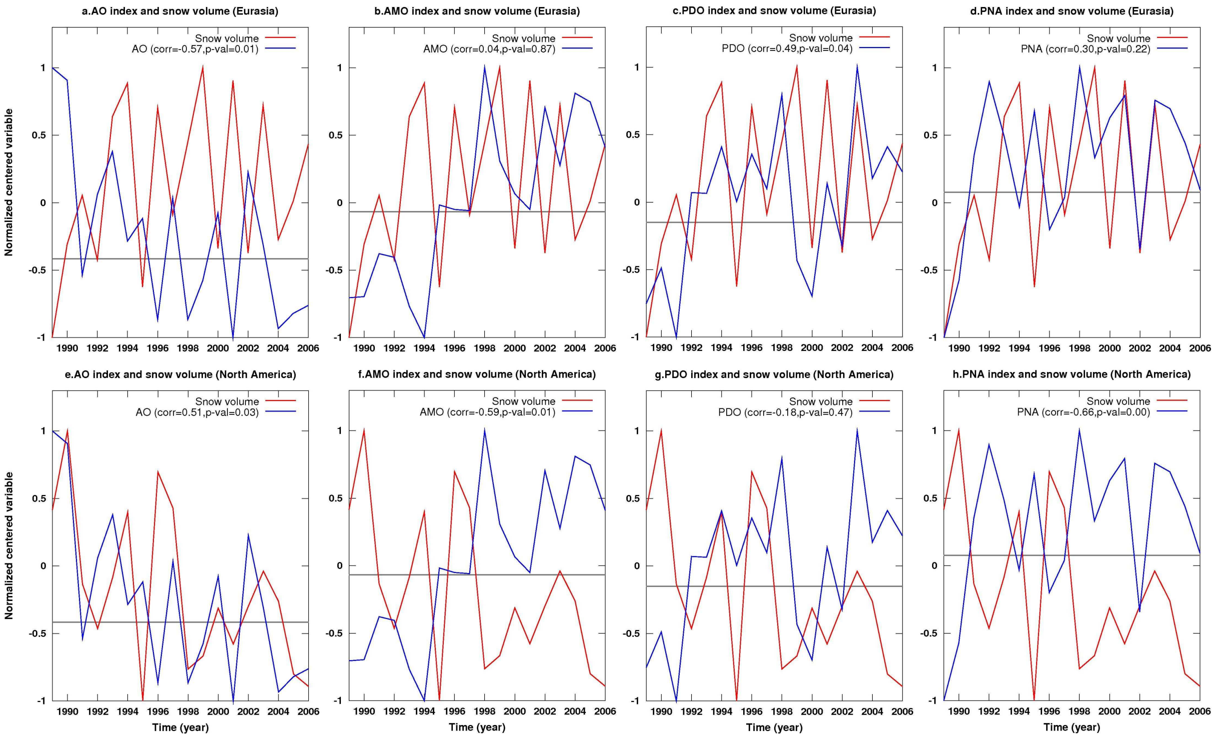

a.AO index and snow volume (Eurasia)
Snow volume
AO (corr=-0.57,p-val=0.01)
b.AMO index and snow volume (Eurasia)
Snow volume
AMO (corr=0.04,p-val=0.87)
c.PDO index and snow volume (Eurasia)
Snow volume
PDO (corr=0.49,p-val=0.04)
d.PNA index and snow volume (Eurasia)
Snow volume
PNA (corr=0.30,p-val=0.22)
e.AO index and snow volume (North America)
Snow volume
AO (corr=0.51,p-val=0.03)
f.AMO index and snow volume (North America)
Snow volume
AMO (corr=-0.59,p-val=0.01)
g.PDO index and snow volume (North America)
Snow volume
PDO (corr=-0.18,p-val=0.47)
h.PNA index and snow volume (North America)
Snow volume
PNA (corr=-0.66,p-val=0.00)
Normalized centered variable
Time (year)

Figure 5:

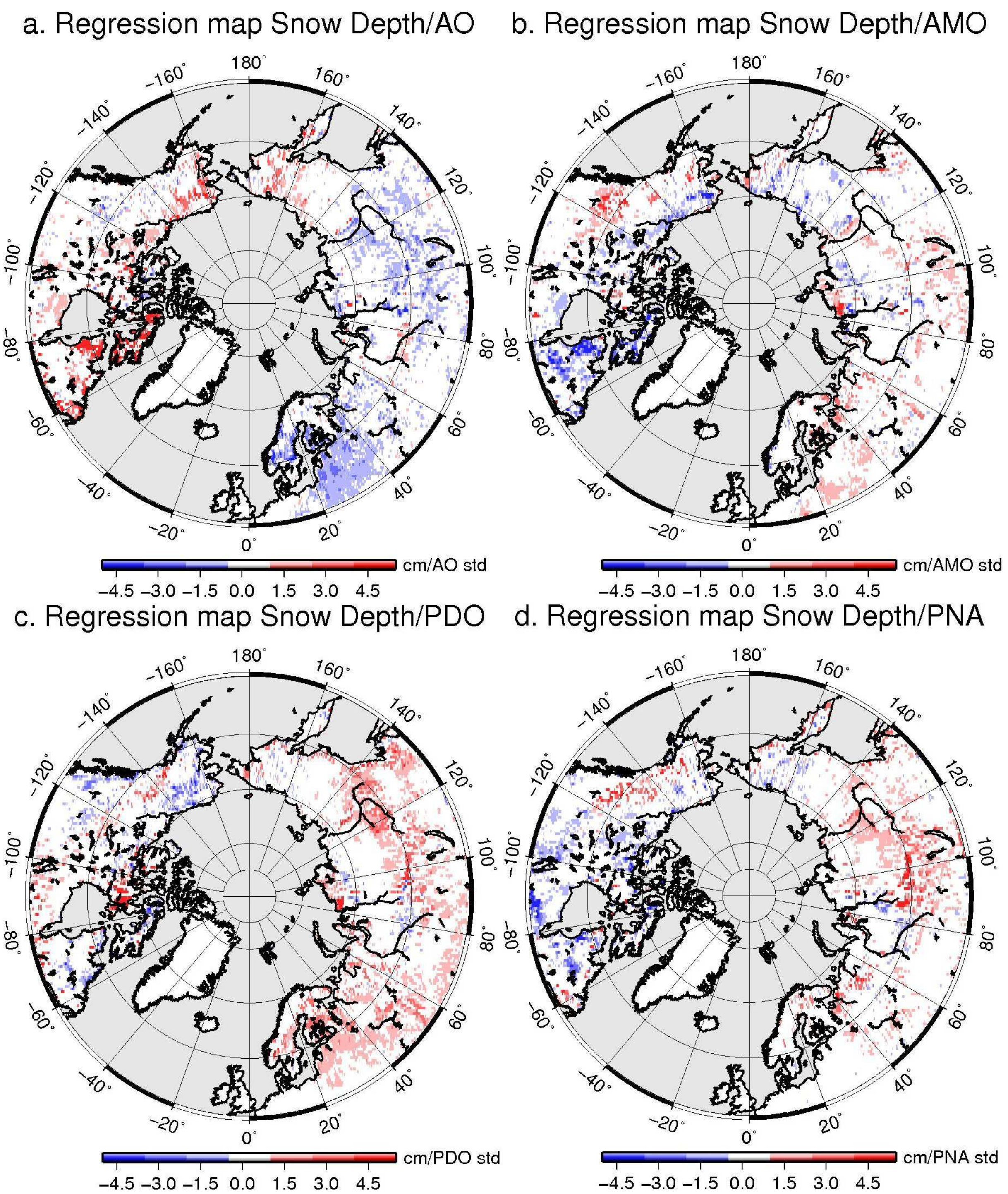
a. Regression map Snow Depth/AO
b. Regression map Snow Depth/AMO
c. Regression map Snow Depth/PDO
d. Regression map Snow Depth/PNA
180°
160°
140°
120°
100°
80°
60°
40°
20°
0°
−20°
−40°
−60°
−80°
−100°
−120°
−140°
−160°
cm/AO std
cm/AMO std
cm/PDO std
cm/PNA std
−4.5 −3.0 −1.5 0.0 1.5 3.0 4.5